Published in final edited form as:
Nat Cell Biol. 2005 September ; 7(9): 901–908.

Phospho-Caveolin-1 Mediates Integrin-Regulated Membrane Domain Internalisation

Miguel A. del Pozo[1,*], **Nazilla B. Alderson**[1], and **Araceli Grande-García**[1]
1*Centro Nacional de Investigaciones Cardiovasculares (CNIC, Spanish National Center for Cardiovascular Research), Madrid 28029, Spain*

Nagaraj Balasubramanian[2] and **Martin A. Schwartz**[2]
2*Departments of Microbiology and Biomedical Engineering, Mellon Prostate Cancer Research Institute and Cardiovascular Research Center, University of Virginia, Charlottesville, Virginia 22908, USA*

William B. Kiosses[3]
3*Microscopy Facility, The Scripps Research Institute, La Jolla, California 92037, USA*

Richard G.W. Anderson[4]
4*Department of Cell Biology, University of Texas Southwestern Medical Center, Dallas, Texas 75235, USA.*

Abstract

Growth of normal cells is anchorage-dependent because signalling through multiple pathways including Erk, PI 3-kinase and Rac requires integrin-mediated cell adhesion [1]. Components of these pathways localize to low density, cholesterol-rich domains in the plasma membrane named “lipid rafts” [2,3] or “cholesterol enriched membrane microdomains” (CEMM) [4]. We previously reported that integrin-mediated adhesion regulates CEMM trafficking such that cell detachment from the extracellular matrix (ECM) triggers CEMM internalisation and clearance from the plasma membrane [5]. We now report that this internalisation is mediated by dynamin-2 and caveolin-1. Internalisation requires phosphorylation of caveolin-1 on tyrosine 14. A shift in localisation of phospho-caveolin-1 from focal adhesions to caveolae induces CEMM internalisation upon cell detachment, which mediates inhibition of Erk, PI 3-kinase and Rac. These data define a novel molecular mechanism for growth and tumour suppression by caveolin-1.

Keywords

anchorage-dependent cell growth; cancer; integrin signalling; caveolin; cholesterol-enriched membrane microdomains (CEMM); Rho GTPases

Loss of anchorage dependence of growth *in vitro* is closely associated with tumour growth and metastasis *in vivo* [1]. The effects of integrins on multiple growth regulatory pathways mediate anchorage-dependence. Conversely, anchorage-independence in cancer cells is due to constitutive activation of these pathways such that integrin-mediated adhesion is no longer

*Correspondence should be addressed to M.A.d.P. (e-mail: madelpozo@cnic.es)

A significant part of this work was performed while some of the authors were located at The Scripps Research Institute, Departments of Immunology (MAdP and NBA, from January 2003 to June 2004) and Cell Biology (MAdP, NBA and WBK until June 2004, and MAS until July 2002), La Jolla, California 92037, USA.

Supplementary Information accompanies the paper on the *Nature Cell Biology*’s website.

Competing Interests statement The authors declare that they have no competing financial interests.

required for signalling. For the small GTPase Rac, a key anchorage-dependent event is translocation of activated protein to the plasma membrane, which is essential for activation of downstream effectors [6]. Regulation by integrins occurs through internalisation of CEMM, which contain Rac plasma membrane binding sites [5]. Internalised CEMM markers include cholesterol, GPI-anchored proteins and GM1, for which approximately 90% was lost from the cell surface [5].

The best defined subtype of CEMM is caveolae, which contain caveolin-1, or in muscle, caveolin-3 [7]. Caveolae are ~100 nm invaginations of the plasma membrane involved in clathrin-independent membrane traffic [8] and intracellular cholesterol transport [9]. Caveolin is a 21 kD protein first identified as a substrate for the v-src tyrosine kinase, which, among several other kinases, phosphorylates caveolin on tyr14 [10,11]. Caveolin is also implicated in modulation of signal transduction. Caveolin inhibits a number of enzymes [11,12] and has been identified as a candidate tumour suppressor [13-16]. Many tumour cells show loss of caveolin expression, and its re-expression reverses anchorage-independent growth [12]. 16% of human breast cancers contain a caveolin mutation [17] and caveolin knockout mice show dramatic acceleration of tumorigenesis in response to carcinogenic stimuli [15,16].

Caveolin is involved in internalisation of GM1 [8]. We therefore investigated the role of caveolin in CEMM internalisation in anchorage-dependent cells after integrin signalling was inactivated by detaching cells from the ECM [1]. When cells were detached, caveolin-1 showed time-dependent movement from the plasma membrane to an intracellular compartment (Fig. 1a; results quantified in 1b) on the same time scale as the raft marker GM1 [5]. This result is consistent with published studies showing that internalised caveolin concentrates in a central region of the cell [18]. Electron microscopy revealed flask-shaped caveolae in the plasma membrane immediately after detachment, but these decreased at later times (Fig. 1c). Quantitation of caveolae confirmed this observation (47.5 caveolae per μm of membrane at 30s; 12.9 at 2h after detachment. Total μm of membrane examined were 29.9 and 29.5 respectively). Immunogold labelling of caveolin-1 in cells shortly after detachment revealed large vacuoles surrounded by invaginated caveolae (Fig. 1d), though these were much less evident at later times (not shown). Similar structures have been previously reported [8]. These results suggest that detachment causes of formation of caveolae-rich membrane internalisation structures. When serum starved, adherent cells were double labelled, caveolin-1 and GM1 were found to significantly co-localize at cell edges (Fig. 2a). Co-localization was similar immediately after detachment (Fig. 2a, quantified in 2b) then increased between 2 and 10 min after loss of adhesion (Fig. 2a), coinciding with internalisation of both GM1 [5] and caveolin-1 (Fig. 1a). Co-localisation of caveolin-1 with GM1 decreased at later times (Fig. 2a,b), suggesting that GM1 is internalised through caveolae and then traffics to a caveolin-1-negative compartment. Thus, detachment induces internalisation of both GM1 and caveolae, suggesting that GM1 internalisation might occur through a caveolin-1-dependent endocytic pathway.

Basal GM1 internalisation proceeds via clathrin-dependent, caveolin-1-dependent, and clathrin and caveolin-1-independent pathways [8]. We therefore characterised the endocytic machinery involved in this integrin-regulated process. Detachment-induced GM1 internalisation was completely abolished in MEFs expressing a dominant negative dynamin-2 mutant (Fig. 2c), but not in MEFs expressing the C-terminal domain of Eps15, a selective inhibitor of the classic clathrin pathway [8,19,20] (Fig. 2d, middle panels). This construct was functional, since it inhibited transferrin receptor internalisation in a parallel assay (Fig. 2e). There is also dynamin-independent, Cdc42-dependent internalisation of GPI-anchored proteins [19]. However, inhibition of Cdc42 with either the Cdc42-binding domain (CBD) of WASP (Fig. 2d, bottom panels) or N17-Cdc42 (not shown) had no effect. These results show that GM1 internalization after detachment is independent of clathrin and Cdc42, but requires dynamin-2.

Since dynamin also mediates caveolin-dependent internalisation [8], these results suggested that caveolin-1 could be involved. To address the requirement for caveolin, tumour lines were screened for caveolin-1 expression. M21L melanoma cells were found to contain no detectable caveolin-1 (Fig 3a), -2, or -3 (not shown). M21L-cav cells in which caveolin-1 was stably expressed were then generated. M21L cells with and without caveolin showed similar morphology, GM1 surface staining and Rac association with membranes when adherent (Supplementary Fig. 1a-c). After detachment, M21L-cav cells resembled NIH-3T3's in that GM1 was cleared from the cell surface (Fig. 3b, top panels). M21L cells, however, retained surface GM1 even after extended incubation in suspension. The two lines had similar intensity of staining after permeabilization (not shown) and similar levels of total GM1 (Supplementary Fig. 1b). Thus, GM1 internalisation also requires caveolin.

Internalisation of CEMM in suspended cells led to loss of GTP-Rac membrane binding and thus blocked its interaction with effectors [5]. We therefore examined the behaviour of V12Rac. Non-adherent M21L cells retained GFP-V12Rac membrane localization, whereas Rac was mainly cytoplasmic in suspended M21L-cav1 cells (Fig. 3b, middle panels). We confirmed this result by measuring pixel intensity of GFP-V12 at cell edges (Fig. 3c) and by biochemical fractionation (Supplementary Fig. 1c). To test Rac effector function, we examined F-actin organization after detachment. Non-adherent M21L cells exhibited asymmetric shapes and F-actin-rich protrusions resembling ruffles (Fig 3b, bottom panels), which are shown more clearly in serial sections (Fig. 3d). These structures were abolished by N17Rac (Supplementary Fig. 1d), demonstrating that they are Rac-dependent. In contrast, M21L-cav cells in suspension were completely round with no surface protrusions (Fig. 3b,d).

To confirm these results, we examined fibroblasts from caveolin-$1^{-/-}$ and caveolin-$1^{+/+}$ littermate mice [21]. These cells showed similar surface staining with CTxB when adherent (not shown), however, detachment triggered loss of cell surface GM1 in caveolin-$1^{+/+}$ (not shown) but not in caveolin$^{-/-}$ fibroblasts (Fig. 4f). Transient transfection with caveolin-1 (Western blot in Fig. 4e) restored the internalisation of GM1 after detachment (Fig 4f, quantified in 4g). Cav$^{-/-}$ fibroblasts also retained GTP-Rac membrane localization and showed actin-rich protrusions in suspension, which were lost after transfection of caveolin (not shown). As an additional assay for Rac function, activation of its effector PAK was assayed. As observed previously, PAK kinase activity was strongly downregulated in suspended WT fibroblasts whereas suspended cav$^{-/-}$ cells retained PAK kinase activity (Fig 3e). Thus, caveolin is required for internalisation of GM1, loss of Rac membrane targeting and subsequent effector interactions upon loss of cell adhesion.

Integrin-mediated adhesion regulates other signalling pathways, including Ras/Erk, FAK and PI3-kinase/Akt [1]. To test whether loss of plasma membrane microdomains influences these pathways, we measured the effect of adhesion in WT and caveolin-$1^{-/-}$ MEFs. Both Erk and Akt were strongly downregulated in non-adherent WT MEFs, whereas activity was retained in suspended caveolin-$1^{-/-}$ cells (Fig. 3f). By contrast, FAK activity was adhesion-dependent in all cases (Fig. 3f). Thus, caveolin is essential for anchorage-dependence of several growth-regulatory pathways but not FAK.

Caveolin-1 is phosphorylated on tyrosine 14 [10,11] and tyrosine phosphorylated caveolin-1 (pY14cav-1) is present in focal adhesions [11,22]. Indeed, phosphocaveolin-1 strongly co-localized with vinculin at focal adhesions and was virtually absent from caveolae marked by caveolin-1 staining in both NIH 3T3 cells (Fig. 4a) and WT MEFs (not shown). Although localization of caveolin-1 to focal adhesions has been previously reported [23], the observed weak staining of focal adhesions with the caveolin-1 antibody suggests that the stoichiometry of caveolin-1 phosphorylation is low. Indeed, western blot densitometry analysis of 1mM vanadate-treated and control NIH 3T3 cells revealed that less than 1% caveolin-1 is

phosphorylated on Tyr 14 (Supplementary Fig. 2). When cells were detached, phosphorylated caveolin-1 became dispersed throughout the plasma membrane where it showed nearly complete co-localization with caveolin-1, in both WT MEFs (Fig. 4b) and NIH 3T3 cells (Supplementary Fig. 3). Co-localization was also observed at later times after detachment in interior regions of the cell (data not shown). The phosphocaveolin-1 antibody showed no staining in detached caveolin-1 deficient MEFs (Fig. 4c), supporting the specificity of the staining pattern. When Triton X-100 extracts were run on sucrose gradients, phosphocaveolin-1 was primarily in the heavy fractions in adherent cells (73±5%) but shifted to the light fractions after detachment (72±7%), consistent with its movement into caveolae. Caveolin Y14 phosphorylation decreased slightly after detachment but this effect was transient and levels recovered after 30-60 min (Fig. 4d). Altogether, these results reveal an increase in caveolae-localized pY14cav-1 upon cell detachment.

Previous studies have linked caveolin phosphorylation to internalisation [8,24,25]. To test whether caveolin Y14 phosphorylation is required for raft internalisation after detachment, $cav^{-/-}$ cells were transfected with Y14F caveolin (Fig. 4e). Expressing cells showed normal levels and cellular distribution of GM1 when adherent (not shown) but in contrast to WT caveolin, detachment failed to trigger internalisation (Fig. 4f; CTxB surface stain quantified in Fig 4g). The Y14F mutant induced normal caveolae in $cav^{-/-}$cells, (Supplementary Fig. 4), demonstrating its functionality. Cav Y14F cells also retained Rac membrane localization and actin-rich membrane protrusions in suspension (not shown, but note morphology in 4f). Thus, tyrosine phosphorylated caveolin is required for raft internalisation and Rac inhibition induced by detachment from the extracellular matrix.

Studies in Cos-7 cells further support this conclusion. These cells showed negligible levels of pY14cav-1 (Fig. 4h) and did not internalise GM1 upon cell detachment (Fig. 4i). Treatment with a low dose (1 μM) of vanadate induced caveolin Y14 phosphorylation to a level similar to 3T3 cells (Fig. 4h). This treatment did not alter GM1 localisation in adherent cells but allowed GM1 internalisation after detachment (Fig. 4i). These results support the hypothesis that pY14cav-1 is required for CEMM internalisation specifically upon loss of cell adhesion.

These data support a model in which, when phospho-caveolin is present in cells at significant levels, it is retained in focal adhesions to prevent internalisation. Cell detachment triggers a shift in phospho-caveolin localization to caveolae, which induces clearance of CEMM and caveolae from the cell surface. Our previous work [5] and the current results suggest that depletion of CEMM from the plasma membrane upon loss of adhesion prevents the activation of multiple signalling pathways required for cell proliferation.

We found previously that the association of Rac with the plasma membrane and activation of effectors downstream of Rac required membrane binding sites that are controlled by integrin-mediated cell adhesion [6]. These binding sites are within CEMM, which are largely cleared from the plasma membrane by internalisation following detachment from the ECM [5]. The present data show first that integrin-regulated CEMM internalisation requires caveolin. In the absence of caveolin, the raft marker GM1 remains on the surface of detached cells, and Rac, Erk and Akt function lose their adhesion-dependence. The transient co-localization of GM1 and caveolin after detachment suggests that internalisation of GM1 proceeds through stimulation of a caveolar endocytosis pathway. Although basal GM1 internalisation proceeds via clathrin-dependent, caveolae-dependent and other endocytic pathways [8,20], our data suggest that internalisation induced by detachment is primarily caveolar. Stimulated raft internalisation in other systems also favours the caveolar route [8]. The observed physical association of integrins with caveolin [26] may be related to these regulatory events.

Second, although caveolin phosphorylation induces internalisation [8,24,25], integrins can inhibit CEMM internalisation by retaining phosphocaveolin in focal adhesions. Phosphocaveolin may, however, have additional functions within the focal adhesions; elucidation of which will be an interesting direction for future work. Detachment from the ECM results in phosphocaveolin localisation to other sites in the plasma membrane where it induces internalisation of CEMM *via* caveolae. Thus, loss of caveolin phosphorylation blocks CEMM internalisation as effectively as complete loss of caveolin. Redistribution of pY14cav-1 may be due to its release from focal adhesions and diffusion to caveolae, and/or to changes in activity or localization of caveolin-1 kinases or phosphatases.

Palazzo et al. have implicated integrins and FAK in regulation of GM1-rich domains [27]. However, in their system other lipid raft markers such as GPI-linked proteins were unaffected. We find that $FAK^{-/-}$ fibroblasts show normal localization of phosphocaveolin-1 to focal adhesion and normal integrin-dependent internalisation of GPI-linked proteins (not shown). Thus, FAK and caveolin-1 appear to mediate two distinct mechanisms of integrin regulation of membrane domains.

In summary, we propose that integrin-mediated adhesion governs the presence of CEMM on the plasma membrane by regulating internalisation through a caveolin-dependent pathway involving changes in phosphocaveolin localization. Caveolin is often mutated in breast cancer [17]. Caveolin-1 null cells show hyperproliferation [21,28], caveolin-1 KO mice show hypertrophy and hyperplasia in several tissues [17,21,28], and loss of caveolin-1 accelerates tumorigenesis [15,16]. While caveolin appears to inhibit some signalling pathways by direct inhibition of signalling enzymes [11,12], our data that caveolin-1 is required for CEMM internalisation provides a novel mechanism for suppression of anchorage independent cell growth by caveolin-1. However, positive effects on cell growth by caveolin-1 have also been described [26]. Whereas caveolin-1 behaves as a tumour suppressor in small cell lung cancers, it promotes survival and growth in non-small cell lung cancers [29]. Thus, caveolin appears to have multiple effects on growth regulatory pathways that show cell type specificity; the mechanism described in this paper is likely to apply in cell types where caveolin-1 suppresses anchorage-independent cell growth. Elucidating the role of caveolin phosphorylation and localization in tumorigenesis is therefore an important goal for future work.

Methods

Cell culture and transfections. NIH 3T3 cells were cultured as described [5]. M21L melanoma cells were maintained in DMEM supplemented with 10 % FBS. MEFs from caveolin-$1^{-/-}$ and caveolin-$1^{+/+}$ littermate mice [21] were grown in DMEM supplemented with 10% fetal bovine serum, glutamine, penicillin and streptomycin. Cells were starved, suspended and transfected as described [5]. M21L cells stably expressing pCDNA3-caveolin-1(1-178)-myc were selected by growth in Geneticin® (Gibco). Transfected cells were screened for protein expression by western blotting with polyclonal anti-caveolin-1 (BD Transduction Labs), mAb anti-myc 9E10 (Santa Cruz Biotechnology, Santa Cruz CA) or anti-flag M2 mAb (Sigma-Aldrich Co., St. Louis, MO).

DNA plasmids and Constructs. Plasmids encoding GFP-tagged N17-Rac, V12-Rac and myc-tagged caveolin-1 were described previously [5,30]. A plasmid encoding flag-tagged caveolin-1 WT and caveolin-1 Y14F were obtained from Dr. C.C. Mastick [10] and subcloned into pCDNA-3. The proper orientation and sequence were verified by sequencing. DNA for transfections was purified by the CsCl gradient method. Dynamin-2 constructs were from Dr. Sandra Schmid (Scripps) and Eps15DIII was from Dr. David Castle (University of Virginia).

Electron Microscopy and immunogold labelling of caveolin-1. Adherent or suspended cells were fixed with 2% glutaraldehyde (EM Sciences, Ft. Washington, PA) in PBS at room temperature for 1 h, post-fixed with 1% osmium tetroxide (OsO_4) in PBS for 1h, and either embedded in Epon, sectioned and viewed with a JEOL 1200EX or processed for immunogold labelling of caveolin-1 following embedding in Lowicryl K4M as described [30].

Immunofluorescence and Confocal Microscopy. Glass coverslips in 24-well plastic dishes were coated with 20 μg/ml human fibronectin or 1 mg/ml poly-L-lysine at 4°C overnight. They were washed three times with PBS, and those coated with FN blocked with 10 mg/ml heat-denatured BSA. Live staining with FITC- or biotinylated-CTxB (1-10 μg/ml) was done at 4° C for 30 min. Rhodamine (TRITC) conjugated-streptavidin (Jackson ImmunoResearch, Inc.) was used to detect biotin. Cells placed in suspension were then attached to poly-L-lysine coated coverslips. Cells were fixed with 2% formaldehyde-PBS for 20 min at 4°C, permeabilized in 0.2% cold Triton X-100 in PBS for 5 min, and blocked with 10 % normal goat serum prior to staining. A pAb to vinculin (sc-5573, Santa Cruz Biotechnology) followed by Texas-Red-conjugated anti-rabbit-IgG (Jackson ImmunoResearch, Inc) was used to stain focal adhesions. Images at the basal Z-section of the cells, close to the substrate were acquired using a Bio-Rad 1024 MRC laser scanning confocal imaging system. Anti-transferrin receptor H68.4 mAb (ATCC) was provided by Dr. David Castle (University of Virginia). Double caveolin-1/pY14cav-1 staining was performed using a rabbit pAb anti-caveolin-1 (BD Transduction Labs) followed by an Alexa 488-conjugated goat anti-rabbit pAb (Molecular Probes) and a mouse anti-pY14cav-1 (BD Transduction Labs) followed by a Rhodamine Red X-conjugated goat anti-mouse pAb (Molecular Probes). Samples were examined with an ultra-spectral confocal microscopy system (Leica TCSSP2-AOBS-UV Leica-Microsystems, Wetzlar, Germany).

PAK kinase assays. PAK was precipitated from cell lysates with polyclonal anti-PAK1 antibody and kinase activity determined using an in-gel kinase assay with myelin basic protein as substrate as described [6]. PAK protein in the precipitates was determined by western blotting with the same antibody. Autoradiographs were quantitated by scanning densitometry and the specific activity (kinase activity normalized to PAK protein) calculated.

Immunoblot analysis of GM1 and phosphorylation of caveolin, Erk, Akt and FAK. Adherent or suspended cells were washed with cold PBS and lysed with RIPA buffer plus protease and phosphatase inhibitors (20 mM Tris pH 7.2, 1% TX-100, 0.5% sodium deoxycholate, 0.1% SDS, 150mM NaCl, 5 mM EDTA, 3 mM EGTA, 10 μg/ml each aprotinin and leupeptin, 1mM PMSF, 10 mM NaF, 20 mM NaH_2PO_4, 10 mM $Na_4P_2O_7$, 1 mM Na_3VO_4, 3 mM β-glycerophosphate). Protein concentrations were quantified using the BCA reagent (Pierce). Equal amounts of samples were analysed by Western blotting with a phospho-caveolin-1 (P-Tyr 14) monoclonal antibody (BD Transduction Labs) and a pAb to caveolin-1. For analysis of surface GM1, M21L and M21L-cav cells were washed with cold PBS, incubated live with 10 μg/ml CTxB (Calbiochem, La Jolla, CA) at 4°C for 30 min, then washed with cold PBS and lysed. Equal amounts of samples were analysed by western blotting. CTxB (55 kD) binding to the cell surface was detected with a goat pAb anti-CTxB (Calbiochem), quantitated by scanning densitometry and normalized to the levels of β1 integrin in the same samples. For analysis of total GM1 (1.5 kD), equal amounts of M21L and M21L-cav cell lysates were analysed by western blotting with HRP-conjugated-CTxB (Sigma). Quantitation and normalization to the levels of β1 integrin was performed as above. To measure activation of integrin-dependent signalling pathways, cell lysates were prepared in the presence of phosphatase inhibitors and analysed by western blot with the following phosphorylation-site specific rabbit pAb: anti-pTpY185/187-Erk1/2 pAb, anti-pS473-Akt pAb, and anti-pY397-FAK (all from Biosource). Blots were then stripped and immunoblotted with phospho-independent antibodies to these proteins, namely anti-Erk1/2 pAb (Biosource), anti Akt pAb

(Cell Signalling), and anti FAK mAb (BD Transduction Labs). Bands were quantitated by scanning densitometry, and the relative amounts of phosphorylated proteins determined.

Binding of Beads. 5 μm polystyrene divinylbenzene beads (Duke Scientific Corporation, Palo Alto, CA) were prepared by washing and incubating with 10 μg/ml fibronectin at 4°C overnight, washed with cold PBS and resuspended by sonication in an ultrasonic bath (Laboratory Supplies Co Inc, Hicksville, NY). Cells were incubated for different times with coated-beads at a cell to bead ratio of 1:40.

Pixel Intensity Profile from Cell Edge. Confocal images of cells expressing GFP V12 Rac were imported into ISEE software. The signal intensity was determined in 5 μm lines from the cell edge toward the cell centre. Average intensity profiles were calculated from 25 regions per cell in 5 different cells per condition.

Co-localization and Distribution of CTxB. Cells were labelled with CTxB-Alexa 568 (Molecular Probes) at 10 μg/ml for 30 min on ice, then kept adherent or placed in suspension and fixed at different times as indicated. Cells were then stained for caveolin-1 followed by anti-mouse Alexa 488 antibody (Molecular Probes). Images were obtained with a BIORAD 1024 scanning laser Confocal Microscope, then imported into Inovison ISEE software, or alternatively recorded with a Zeiss LSM510 laser Confocal Microscope, then analysed using the Metamorph Imaging System (version 6.3). Individual cells (overlayed image of both wavelengths) were mapped and pasted into a new image file. The individual images recorded following excitation at both wavelengths (568 nm for GM1 and 488 nm for caveolin-1) were then separated and a lower threshold was set individually for each image to ensure that background fluorescence was reduced to zero. The thresholded (background subtracted) images were then analysed using the quantitative co-localization function of the Metamorph software. The total pixel intensity of the thresholded caveolin-1 that co-localized with GM1 was quantitated and displayed as a percent of the total pixel intensity of caveolin-1 staining over the entire cell. This method was used for 10 cells per condition from three separate experiments.

Quantitation of caveolin-1 translocation. Confocal images of cells stained for endogenous caveolin-1 were imported into Inovison ISEE software. Using this software, a line was drawn by hand around the periphery of each cell, then a second line was drawn ~3.5 μm inside the first line to divide the cell into *exterior* and *interior* zones. Average fluorescence intensity was obtained within each subcellular region for 10 cells per condition.

Quantitation of GM1 cell surface fluorescence intensity. Using ISEE Unix software, CTxB-FITC-surface labelled cells were outlined and the average fluorescence intensity for the entire cell determined for 10 cells per condition.

Vanadate treatment. 2×10^5 NIH- 3T3 or COS-7 cells were plated in 6 well plates, then incubated with or without 1μm sodium pervanadate (sodium orthovanadate activated with 1:1000 diluted H_2O_2 during 30 min).

Supplementary Material

Refer to Web version on PubMed Central for supplementary material.

Acknowledgements

Acknowledgements. We thank Drs. M. P. Lisanti for the caveolin-1 null MEFs, C.C. Mastick for the caveolin Y14F vector, Sandra Schmid for the dynamin constructs, David Castle for the Eps15DIII mutant and H68.4 mAb, Nahum Meller for the Cdc42 inhibitor CBD-WASP, Wei-Ping Li, Yunshu Ying and Jan Redick for assistance in EM analysis, María C. Montoya and Diego Megías for assistance with the Leica ultra-spectral confocal microscope, E.M. Moreno

for technical assistance, and S. Schmid, M. Ginsberg, S. Shattil and K. Ley for critical reading of the manuscript. This work was supported by MEC (Spanish Ministry of Science and Education) through grants SAF2002-0245 and GEN2003-20239-C06-04 to M.A.d.P., a predoctoral fellowship (BEF-2003-2712, to A.G.-G.), and the Ramón y Cajal Program (to M.A.d.P.); and by EUROHORCS (European Heads Of Research Councils) and European Science Foundation (ESF) through a EURYI (European Young Investigator) Award to M.A.d.P.; USPHS grant RO1 GM47214 to M.A.S.; and grants from NIH and the Perot Family Foundation to R.G.W.A.

References

1. Schwartz MA. Integrins, oncogenes, and anchorage independence. J. Cell Biol 1997;139:575–578. [PubMed: 9348275]
2. Edidin M. The state of lipid rafts: from model membranes to cells. Annu Rev Biophys Biomol Struct 2003;32:257–83. [PubMed: 12543707]
3. Lagerholm BC, Weinreb GE, Jacobson K, Thompson NL. Detecting Microdomains in Intact Cell Membranes. Annu Rev Phys Chem 2005;56:309–336. [PubMed: 15796703]
4. Grande A, Echarri A, del Pozo MA. Integrin regulation of membrane domain trafficking and Rac targeting. Biochemical Society Transactions 2005;33:609–613. [PubMed: 16042555]
5. del Pozo MA, et al. Integrins regulate Rac targeting by internalization of membrane domains. Science 2004;303:839–42. [PubMed: 14764880]
6. del Pozo MA, Price LS, Alderson NB, Ren XD, Schwartz MA. Adhesion to the extracellular matrix regulates the coupling of the small GTPase Rac to its effector PAK. Embo J 2000;19:2008–2014. [PubMed: 10790367]
7. Parton RG. Caveolae--from ultrastructure to molecular mechanisms. Nat Rev Mol Cell Biol 2003;4:162–7. [PubMed: 12563293]
8. Pelkmans L, Puntener D, Helenius A. Local actin polymerization and dynamin recruitment in SV40-induced internalization of caveolae. Science 2002;296:535–9. [PubMed: 11964480]
9. Fielding CJ, Fielding PE. Caveolae and intracellular trafficking of cholesterol. Adv Drug Deliv Rev 2001;49:251–64. [PubMed: 11551398]
10. Cao H, Courchesne WE, Mastick CC. A phosphotyrosine-dependent protein interaction screen reveals a Role for phosphorylation of caveolin-1 on tyrosine 14: Recruitment of C-terminal Src kinase. J Biol Chem 2002;22:22.
11. Lee H, et al. Constitutive and growth factor-regulated phosphorylation of caveolin-1 occurs at the same site (Tyr-14) in vivo: identification of a c-Src/Cav-1/Grb7 signaling cassette. Mol Endocrinol 2000;14:1750–75. [PubMed: 11075810]
12. Engelman JA, et al. Recombinant expression of caveolin-1 in oncogenically transformed cells abrogates anchorage-independent growth. J. Biol. Chem 1997;272:16374–16381. [PubMed: 9195944]
13. Fiucci G, Ravid D, Reich R, Liscovitch M. Caveolin-1 inhibits anchorage-independent growth, anoikis and invasiveness in MCF-7 human breast cancer cells. Oncogene 2002;21:2365–75. [PubMed: 11948420]
14. Wiechen K, et al. Caveolin-1 is down-regulated in human ovarian carcinoma and acts as a candidate tumor suppressor gene. Am J Pathol 2001;159:1635–43. [PubMed: 11696424]
15. Capozza F, et al. Absence of caveolin-1 sensitizes mouse skin to carcinogen-induced epidermal hyperplasia and tumor formation. Am J Pathol 2003;162:2029–39. [PubMed: 12759258]
16. Williams TM, et al. Caveolin-1 gene disruption promotes mammary tumorigenesis and dramatically enhances lung metastasis in vivo. Role of Cav-1 in cell invasiveness and matrix metalloproteinase (MMP-2/9) secretion. J Biol Chem 2004;279:51630–46. [PubMed: 15355971]
17. Lee H, et al. Caveolin-1 mutations (P132L and null) and the pathogenesis of breast cancer: caveolin-1 (P132L) behaves in a dominant-negative manner and caveolin-1 (-/-) null mice show mammary epithelial cell hyperplasia. Am J Pathol 2002;161:1357–69. [PubMed: 12368209]
18. Murata M, et al. VIP21/caveolin is a cholesterol-binding protein. Proc Natl Acad Sci U S A 1995;92:10339–43. [PubMed: 7479780]
19. Sabharanjak S, Sharma P, Parton RG, Mayor S. GPI-anchored proteins are delivered to recycling endosomes via a distinct cdc42-regulated, clathrin-independent pinocytic pathway. Dev Cell 2002;2:411–23. [PubMed: 11970892]

20. DammEMClathrin- and caveolin-1-independent endocytosis: entry of simian virus 40 into cells devoid of caveolae. J Cell Biol200516847788Epub 2005 Jan 24 [PubMed: 15668298]

21. Razani B, et al. Caveolin-1 null mice are viable but show evidence of hyperproliferative and vascular abnormalities. J Biol Chem 2001;276:38121–38. [PubMed: 11457855]

22. Mettouchi A, et al. Integrin-specific activation of Rac controls progression through the G(1) phase of the cell cycle. Mol Cell 2001;8:115–27. [PubMed: 11511365]

23. Boyd ND, Chan BM, Petersen NO. Beta1 integrins are distributed in adhesion structures with fibronectin and caveolin and in coated pits. Biochem Cell Biol 2003;81:335–48. [PubMed: 14569297]

24. Parton RG, Joggerst B, Simons K. Regulated internalization of caveolae. J Cell Biol 1994;127:1199–215. [PubMed: 7962085]

25. Aoki T, Nomura R, Fujimoto T. Tyrosine phosphorylation of caveolin-1 in the endothelium. Exp Cell Res 1999;253:629–36. [PubMed: 10585286]

26. Wary KK, Mariotti A, Zurzolo C, Giancotti FG. A requirement for caveolin-1 and associated kinase Fyn in integrin signaling and anchorage-dependent cell growth. Cell 1998;94:625–634. [PubMed: 9741627]

27. Palazzo AF, Eng CH, Schlaepfer DD, Marcantonio EE, Gundersen GG. Localized stabilization of microtubules by integrin- and FAK-facilitated Rho signaling. Science 2004;303:836–9. [PubMed: 14764879]

28. Drab M, et al. Loss of caveolae, vascular dysfunction, and pulmonary defects in caveolin-1 gene-disrupted mice. Science 2001;293:2449–52. [PubMed: 11498544]

29. Sunaga N, et al. Different roles for caveolin-1 in the development of non-small cell lung cancer versus small cell lung cancer. Cancer Res 2004;64:4277–85. [PubMed: 15205342]

30. Machleidt T, Li WP, Liu P, Anderson RG. Multiple domains in caveolin-1 control its intracellular traffic. J. Cell Biol 2000;148:17–28. [PubMed: 10629215]

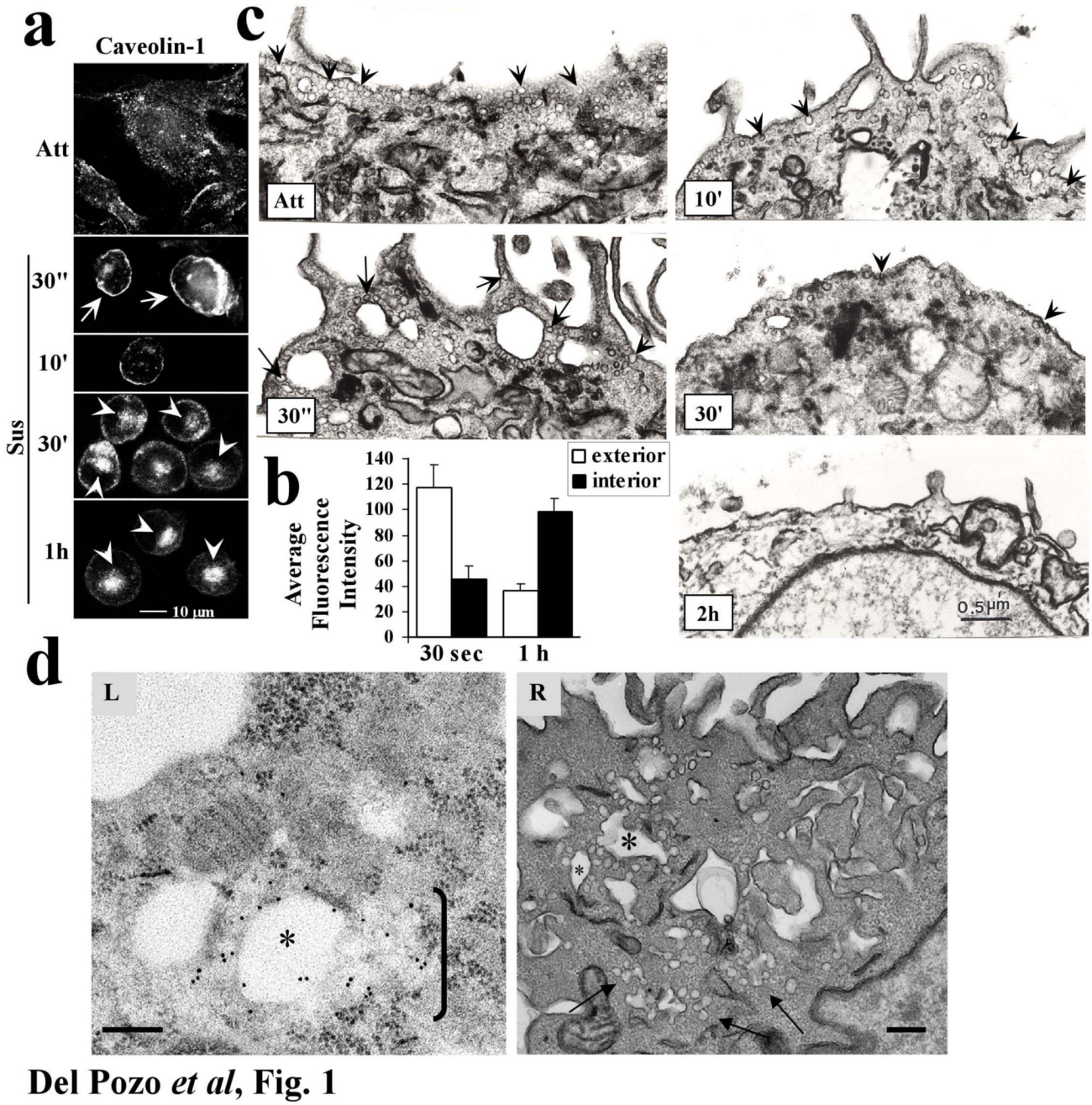

Figure 1.

Caveolin-1 internalisation. (a) Adherent 3T3 cells or cells suspended for the indicated times were fixed, permeabilized and stained for caveolin-1. Cell surface (arrows) *vs.* intracellular (arrowheads) staining is indicated. **(b)** Internalisation of caveolin in images from (a) was quantified as described in Methods. Caveolin fluorescence within 3.5 microns of the cell surface is considered exterior; fluorescence internal to this zone, further from the plasma membrane, is considered interior. Values are means ± S.E.M. from 10 cells in 3 independent experiments. Differences between 30s and 1h are statistically significant ($p<2.5\times10^{-4}$ for the interior region and $p<7\times10^{-3}$ for the exterior). **(c)** Attached cells or cells suspended for the indicated times were fixed and processed for electron microscopy to detect caveolae in the

plasma membrane. Caveolae are indicated by arrows. Images are representative of areas within cells where caveolae are concentrated. **(d)** Cells suspended for 2 min. were fixed and processed for either (L) immunogold labelling of caveolin-1 or (R) electron microscopy. (L) A region of caveolae internalisation showing a vacuole surrounded by multiple α-Cav-1 IgG gold particles. To the right of this vacuole (bracket) is a cluster of caveolae emanating from the vacuole. (R) A similar region of a cell processed for regular TEM microscopy. This image shows several caveolae-rich vacuoles (asterisks) and associated clusters of caveolae and caveolae-derived vesicles (arrows). Bar=0.2 μm. (n=3).

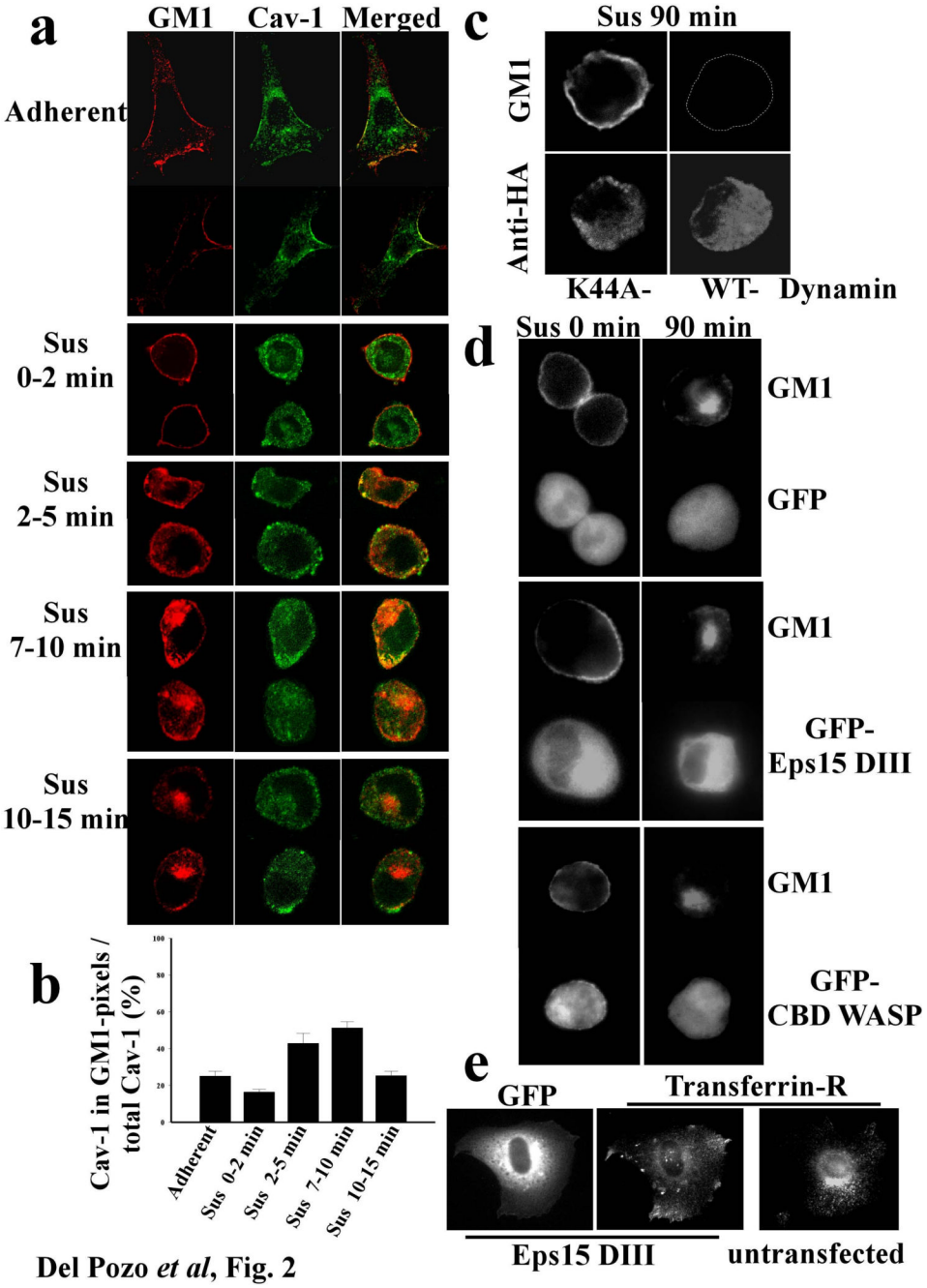

Figure 2.

Pathway of integrin-regulated GM1 internalisation. (a) Serum deprived NIH-3T3 fibroblasts were surface labelled on ice with CTxB-Alexa 568, detached and held in suspension (Sus) for the indicated times, or plated on FN for 2hours (Adherent). Cells were then fixed and stained for caveolin-1 in green. Cells shown are observed at the equatorial plane and representative of up to 50 cells at each time point. **(b)** To quantify co-localization between GM-1 and caveolin, pixels that were positive for GM1 stain were identified and the fraction of the caveolin-1 stain within these zones calculated. Values are means ± S.E.M. from 3 independent experiments. **(c)** $_{WT}$ MEFs expressing HA-tagged dominant negative (K44A) or $_{WT}$ dynamin-2 were held in suspension for 90 min, surface labelled with Alexa 488-CTxB, and

then stained with anti-HA antibody. **(d)** WT MEFs expressing GFP alone, GFP-tagged Eps15DIII, or the Cdc42-binding domain (CBD) of WASP were surface labelled with Alexa 568-CTB, then detached and held in suspension for the indicated times. **(e)** Control and GFP-tagged Eps15DIII expressing WT MEFs adherent on FN were stained for the transferrin receptor. Cells shown are representative of three independent experiments.

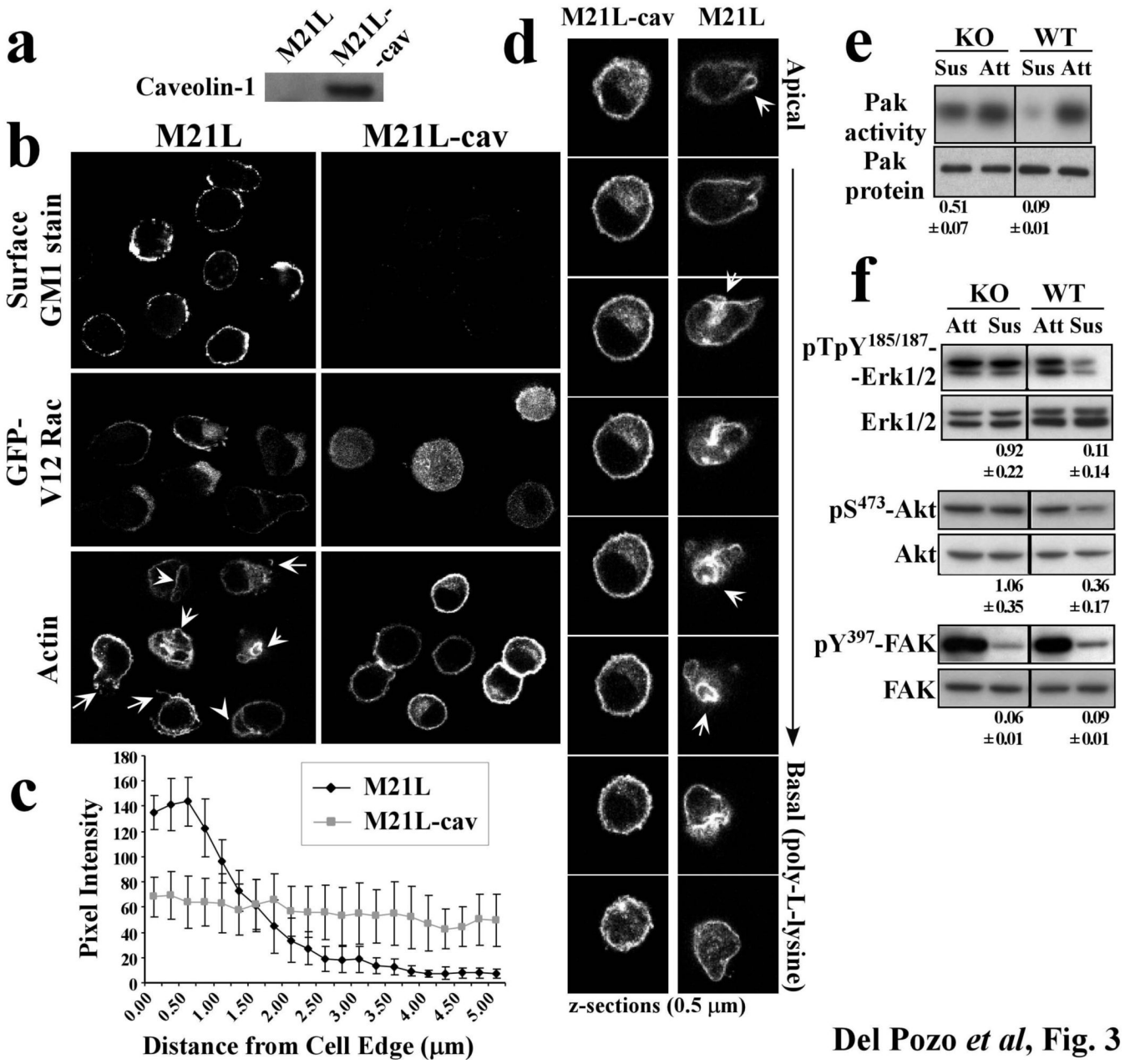

Figure 3.

Requirement for Caveolin-1. (a) Lysates from M21L melanoma or M21L-cav cells were analysed by Western blotting with anti-caveolin polyclonal Ab. **(b)** Cells detached for 2h (top panels) were stained live with FITC-CTxB to label surface GM1. Middle panels: cells expressing GFP-V12Rac. Bottom panels: Cells stained with rhodamine-phalloidin. Arrows indicate protrusions and ruffle-like structures **(c)** GFPV12Rac localization to the membrane in (b) was assessed by measuring pixel intensity starting at the cell edge. Values are means ± SEM. **(d)** Confocal z-section series of actin-stained cells. **(e)** Serum-starved caveolin-1$^{-/-}$ MEFs (KO) or caveolin-1$^{+/+}$ MEFs (WT), adherent or suspended for 2h, were stimulated with 10% serum for 10 min, and PAK kinase activity assayed. **(f)** Caveolin-1$^{-/-}$ MEFs (KO) or caveolin-1$^{+/+}$ MEFs (WT) were kept adherent or suspended for 8h in the presence of 10% serum. Cell lysates were analysed by Western blotting with phospho-specific antibodies to

Erk1/2, Akt, and FAK, or with phospho-independent antibodies to the same proteins for normalization. Values in (e) and (f) are means ± S.D. of the specific enzymatic activity (kinase activity or amount of phospho-protein normalized to total protein) in non-adherent cells normalized to that of adherent cells (n=4).

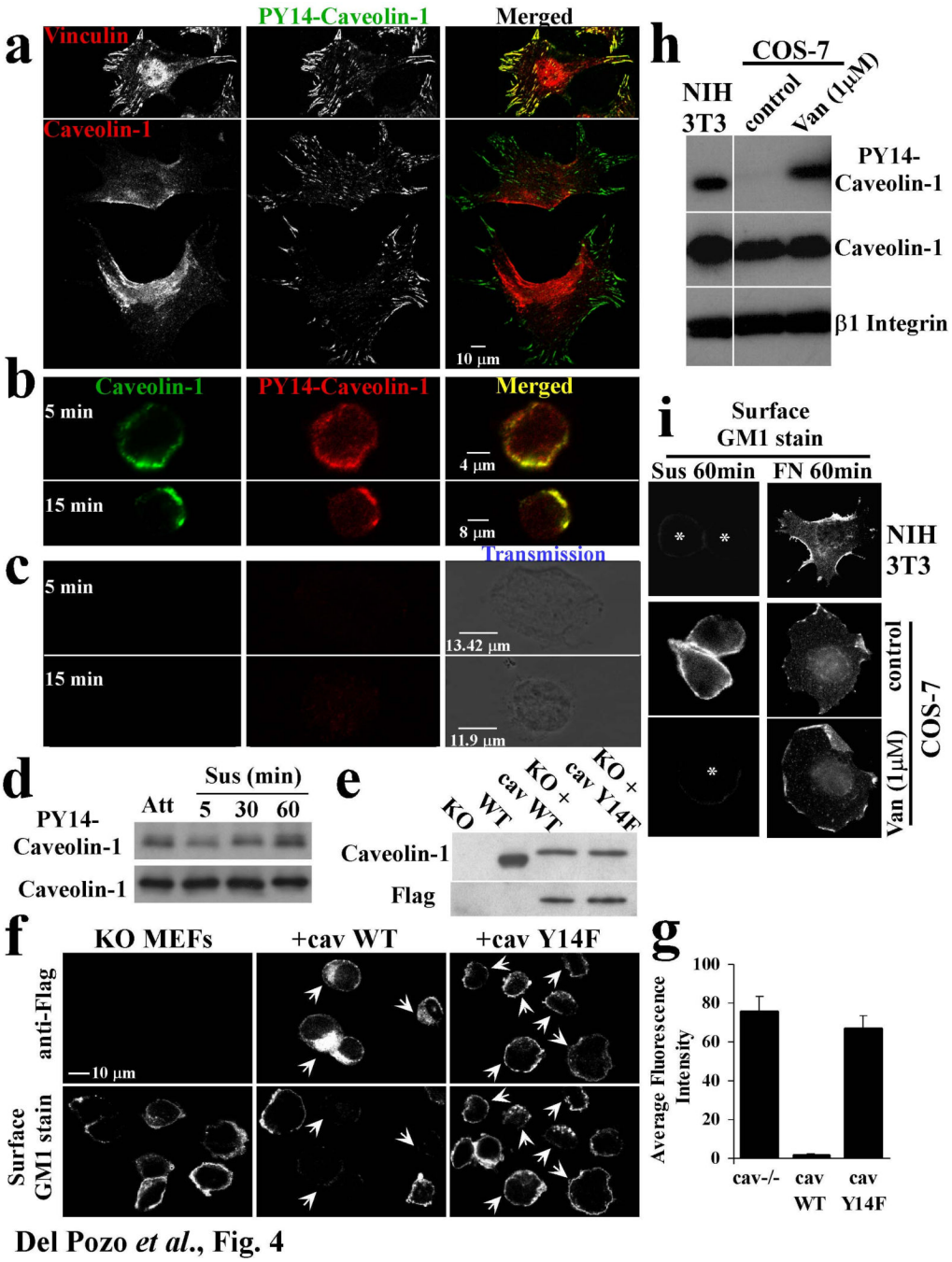

Figure 4.

Phospho-caveolin-1 mediates integrin-dependent membrane domain internalisation.

(a) Adherent NIH-3T3 cells were doubly stained for phospho-caveolin-1 plus either vinculin or total caveolin-1. WT MEFs **(b)** or caveolin-1$^{-/-}$ MEFs **(c)** in suspension were stained for total caveolin-1 plus pY14cav-1. **(d)** NIH-3T3 cells were kept adherent or placed in suspension for the indicated times. Cell lysates were analysed by Western blotting with anti-caveolin-1 or anti-phosphocaveolin-1 (n=10). **(e)** Western blotting for caveolin-1 and flag in caveolin-1 $^{+/+}$ MEFs (WT), caveolin-1 $^{-/-}$ MEFs (KO), and KO MEFs transiently transfected with flag-tagged WT or Y14F caveolin-1. **(f)**. Caveolin-null MEFs transiently transfected with WT or Y14F caveolin-1 were detached for 2h and stained live with FITC-CTxB to label surface

GM1, then fixed and stained with anti-flag mAb to detect caveolin expression. Arrows denote transfected cells. Images are single confocal sections (n=4). **(g)** Quantitation of surface GM1. The level of surface GM1 was quantified by measuring total staining intensity of suspended, surface CTxB-labelled untransfected caveolin-null cells and cells expressing WT or Y14F caveolin from (f). Values are means ± S.E.M. from 10 cells in 4 independent experiments. **(h)** NIH-3T3 cells, untreated COS-7 cells, and COS-7 cells incubated with 1μM sodium pervanadate for 1 h were lysed, and analysed by western blotting with antibodies against caveolin-1, pY14cav-1, and β1 integrin. **(i)** Adherent and suspended cells treated as in (h) were surface labelled with CTxB-Alexa 568. Asterisks denote cells not readily visible due to low surface labelling. Results are representative of three independent experiments.